Contents lists available at ScienceDirect

Spectrochimica Acta Part A: Molecular and Biomolecular Spectroscopy

journal homepage: www.elsevier.com

Spectroscopic and SEM evidences for G4-DNA binding by a synthetic alkyne-containing amino acid with anticancer activity

Marta A. Fik-Jaskółka [a, b, c, 1], Anna F. Mkrtchyan [d, e, 1], Ashot S. Saghyan [d, e], Rosanna Palumbo [c], Agnieszka Belter [f], Liana A. Hayriyan [d, e], Hayarpi Simonyan [e], Valentina Roviello [g], Giovanni N. Roviello [c, *]

[a] Department of Bioinorganic Chemistry, Faculty of Chemistry, Adam Mickiewicz University in Poznań, Uniwersytetu Poznańskiego Str. 8, 61-614 Poznan, Poland
[b] Centre for Advanced Technologies, Adam Mickiewicz University in Poznań, Uniwersytetu Poznańskiego Str. 10, 61-614 Poznań, Poland
[c] Istituto di Biostrutture e Bioimmagini IBB - CNR, Via Mezzocannone 16, I-80134 Naples, Italy
[d] Scientific and Production Center "Armbiotechnology" of NAS RA, 14 Gyurjyan Str., 0056 Yerevan, Armenia
[e] Institute of Pharmacy, Yerevan State University, 1 Alex Manoogian Str., 0025 Yerevan, Armenia
[f] Institute of Bioorganic Chemistry, Polish Academy of Sciences, Noskowskiego 12/14, 61-704 Poznan, Poland
[g] Department of Chemical, Materials and Industrial Production Engineering (DICMaPI), University of Naples Federico II, Piazzale V. Tecchio 80, 80125 Naples, Italy

ARTICLE INFO

Article history:
Received 16 October 2019
Received in revised form 26 November 2019
Accepted 1 December 2019
Available online xxx

Keywords:
Unnatural amino acids
Copper-binding
Ni(II)-complex intermediates
Anticancer drugs
DNA quadruplex, telomeric DNA
C-myc
BSA

ABSTRACT

Herein, we present a spectroscopic (CD and UV) and SEM study of a phenylalanine derivative carrying a terminal alkyne moiety and indicated by us CF3IIIPhe, with particular attention to its interaction with Cu(II) cation and some biological macromolecules, as well as a preliminary evaluation of its effect on cancerous cells. CD spectroscopy evidenced the ability of CF3IIIPhe to interact with tel_{26} and c-myc, two quadruplex DNA (G4 DNA) models explored in this study. Other CD and UV studies revealed the ability of the unnatural amino acid to form aggregates in aqueous solution, bind Cu(II) cation, and interact with a serum albumin (BSA). Cellular studies demonstrated CF3IIIPhe antiproliferative activity on PC3 cells. Its ability to bind telomeric DNA was verified with tel_{26} by CD investigation and SEM analysis, that revealed a noteworthy change in DNA morphology (mainly based on nanosphere structures) by CF3IIIPhe, confirming its G4-DNA binding ability already evidenced by spectroscopy.

1. Introduction

Among the several classes of synthetic molecules investigated so far as novel therapeutic agents, unnatural amino acids have been almost unexplored. In fact, chemically synthesized non-proteinogenic amino acids are generally utilized as building blocks for the realization of peptidic- or non-peptidic drugs [1–3] also in conjugation with DNA bases, forming nucleobase-bearing amino acids and peptides [4–6]. However, the scientific literature on synthetic amino acids studied as bioactive compounds and not as constituent of peptides or other more complex structures is still very limited. For example, we previously reported on synthetic aromatic amino acid derivatives that showed RNA binding ability and anticancer activity towards PC3 prostate cancer cells [7–9]. Other remarkable properties were reported recently by Răsădean et al. [10] for amino acid derivatives containing aromatic moieties acting as versatile binders of G4 DNAs, molecular systems of great biomedical relevance that have been often proposed as targets in anticancer strategies [11] as well as aptamers, due to their ability to interact with proteins [12]. This study attracted much interest because it opened the door to the exploration of aromatic amino acid structures as G4 DNA ligands. Hence, aiming at contributing to this theme and, more in general, at investigating the potential of synthetic amino acids as anticancer drugs, we have directed our efforts towards screening novel chemical modifications into amino acid scaffolds which led to the synthesis of CF3IIIPhe, i.e. an acetylenic L-phenylalanine derivative containing a trifluoromethyl moiety in the p-position of the aromatic ring (Fig. 1).

In fact, it was reported that the incorporation of a trifluoromethyl group in a structure leads to enhanced lipophilicity and bioavailability of the potential drug [13–16]. Besides, triple bond derivatization was associated to bioactive alkyne-containing amino acids [17] and acetylenic anticancer agents [18].

In the designed molecule, aryl and acetylene moieties laid apart each other as ascertained by computer assisted studies (Figs. S1 and S2), remaining, thus, free to interact, e.g. via hydrophobic and aromatic interactions, with biomolecular targets.

Particular attention was paid in this work to the spectroscopic study of the interaction of CF3IIIPhe with telomeric and c-myc DNAs. These are typically studied as G4 DNA models because provide different and well-characterized topologies under specific exper-

* Corresponding author.
Email address: giroviel@unina.it, giovanni.roviello@cnr.it (G.N. Roviello)
[1] These authors equally contributed to this work.

https://doi.org/10.1016/j.saa.2019.117884
1386-1425/

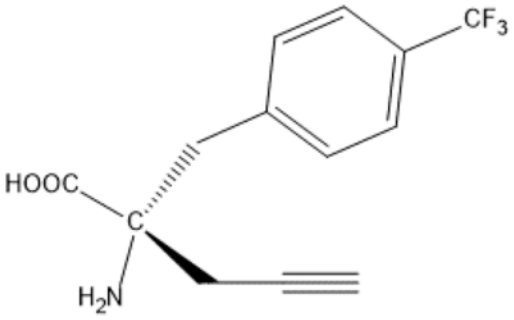

Fig. 1. Structure of the alkyne-containing amino acid CF3IIIPhe.

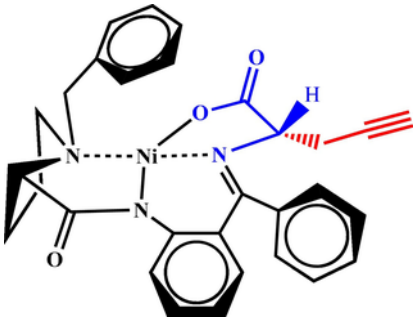

Fig. 2. The structure of (*S*)-BPB-Ni-(*S*)-PGly complex.

imental conditions. Moreover, both are DNAs of biomedical importance as their interaction with drugs can determine desirable anticancer effects [11]. In fact, while telomeric DNA binders may block the habit found in most human cancer cells to infinitely replicate becoming immortal, c-myc ligands target a promoter quadruplex, present upstream of the proto-oncogene myc, down-regulating, thus, oncoprotein overexpression [19,20]. However, other properties emerged by our study including the anticancer activity on PC3 of the alkyne-containing amino acid, as well as the possibility to complex Cu(II) cation and form aggregates in aqueous solution, as illustrated in the sections below.

2. Experimental

2.1. Materials and methods

The alkyl halogenide was obtained from commercial sources and used without further purification. The initial Ni^{II}-(*S*)-BPB-(*S*)-PGly complex was prepared from following literature protocols [21]. TLC analyses were performed on glass plates coated with silica gel 60 F254. Column chromatography was performed on silica gel (60 × 120 mesh) on a glass column. Melting points (mp) were determined by "Elektrothermal". ^{1}H and ^{13}C NMR spectra ("Mercury-300 Varian" 300 MHz respectively) were recorded using TMS as an internal standard (0 ppm). Elemental analyses were done by elemental analyzer EURO EA 3000. The enantiomeric purity of the amino acid was determined by HPLC ("Waters Alliance 2695 HPLC System") on the chiral phase Diaspher-110-Chirasel-E-PA 6:0 mkm 4.0 × 250 mm, and a mixture of 20% of MeOH and of 80% of a 0:1 M aqueous solu-

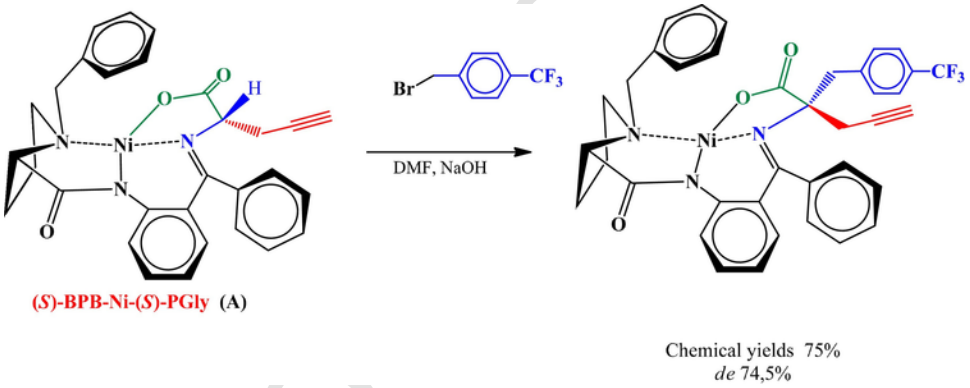

Scheme 1. C-alkylation of amino acid α-position of the (*S*)-BPB-Ni-(*S*)-PGly complex.

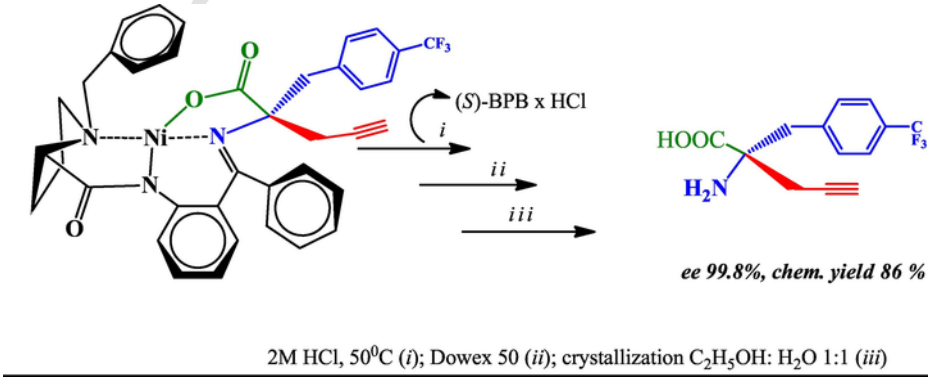

Scheme 2. Synthetic route to CF3IIIPhe.

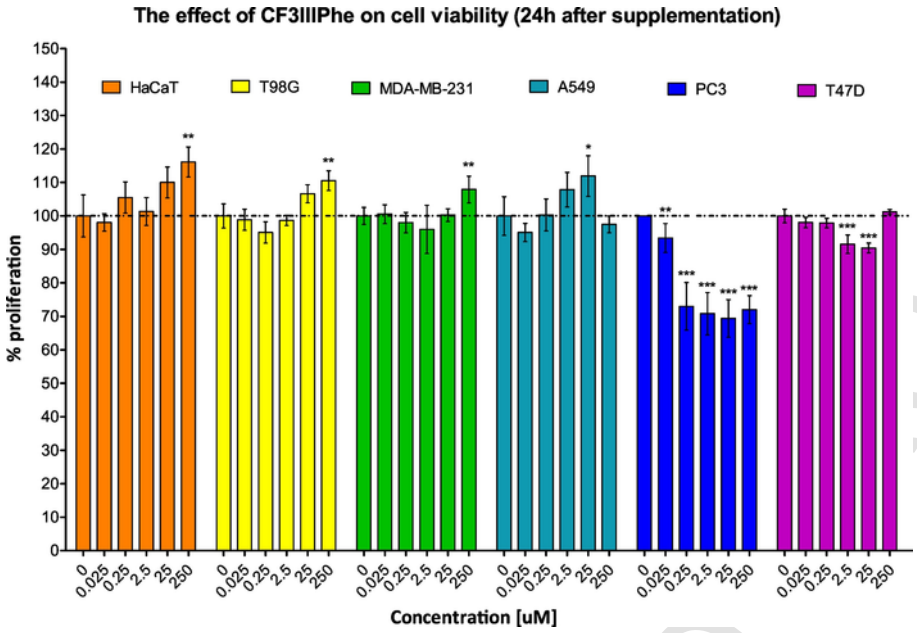

Fig. 3. The effect of CFIIIPhe on cancer (T98G, A549, MDA-MB-231, A47D, PC3) and nontumorigenic (HaCaT) cell lines. Cells were treated at the concentration indicated for 24 h. Cell viability was determined by MTT assay (HaCaT, T98G, MDA-MB-231, A547, T47D cells) or CCK-8 assay (PC3 cells). Values are means ± SE of at least three independent experiments. Significance of changes in cell viability was determined with ANOVA analysis (Table S2). p values of 0.05 were used as the limit for statistical significance. * - $p<0,05$, ** - $p<0,001$, *** - $p<0,0001$.

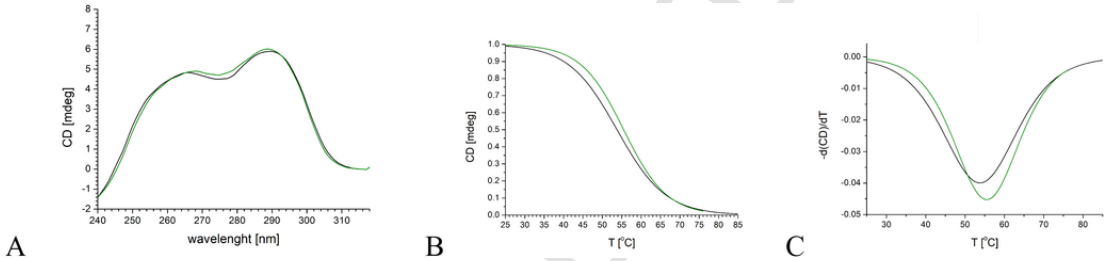

Fig. 4. CD binding experiment on tel_{26} + CF3IIIPhe in 10 mM TrisHCl, 100 mM KCl, pH 7.4: CD spectra of telomeric DNA alone and in the presence of (A); normalized CD melting curves relative to tel_{26} and its complexes with CF3IIIPhe (B); first derivatives of CD melting sigmoids for T_m determination of tel_{26} and its complex with CF3IIIPhe (C). – (DNA + CF3IIIPhe), – (DNA alone).

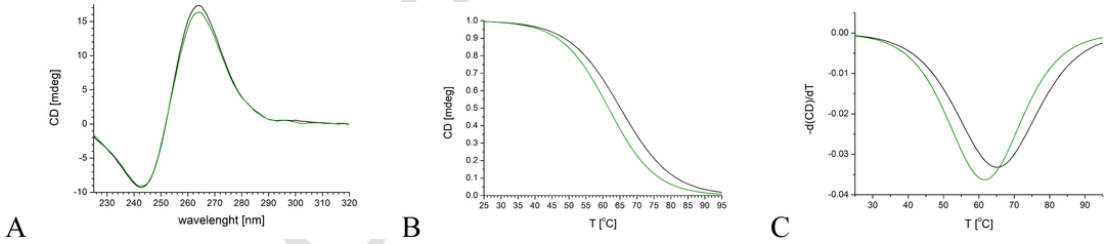

Fig. 5. CD binding experiment on c-myc + CF3IIIPhe in 1 × PBS, pH 7.4: CD spectra of c-myc DNA alone and in the presence of CF3IIIPhe (A); normalized CD melting curves of c-myc and its complex with CF3IIIPhe (B); first derivative of CD melting sigmoids for determination of T_ms relative to c-myc and its complex with CF3IIIPhe (C). – (DNA + CF3IIIPhe), – (DNA alone).

Table 1
Stabilization effect on tel_{26} by CF3IIIPhe in 10 mM TrisHCl, 100 mM KCl, pH 7.4.

Sample	T_m [°C] ± SE
tel_{26}	53.8 ± 0.2
tel_{26} + CF3IIIPhe	55.4 ± 0.2

Table 2
Destabilization effect on c-myc by CF3IIIPhe in 1× PBS, pH 7.4.

Sample	T_m [°C] ± SE
c-myc	65.2 ± 0.2
c-myc + CF3IIIPhe	61.6 ± 0.2

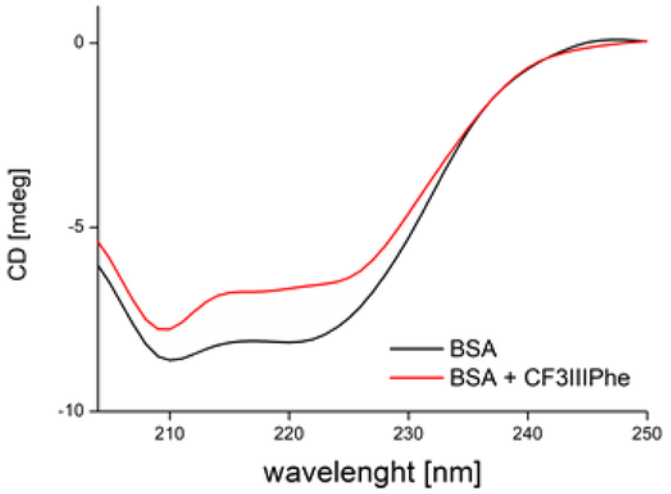

Fig. 6. CD studies on BSA binding of CF3IIIPhe: – BSA alone; – BSA + CF3IIIPhe, 1× PBS buffer (pH 7.4), 15 °C.

tion of $NaH_2PO_4 \times 2H_2O$ was used as the eluent. The optical rotation was measured on a Perkin Elmer-341 polarimeter. In the present work the value of optical rotation of the diastereomeric complex synthesized had a positive value at 589 nm, which is an evidence of (*S*)-absolute configuration of the amino acid moiety derived from the major diastereomeric complex. This was also shown by chiral HPLC analysis of the isolated amino acid. For this comparison, the racemic (*S*;*R*) mixture was synthesized and analyzed, followed by the sample obtained in the present work. Racemate sample was obtained by the same method, i.e. by using a similarly structured complex of achiral *N*-(2-benzoylphenyl)pyridine-2-carboxamide (PBP) auxiliary instead of the complex of an chiral (*S*)-BPB, which resulted in racemate mixture of amino acid. Therefore, according to the data of optical rotation of the diastereomeric complex at 589 nm and chiral HPLC analysis of final amino acids, the (*S*,*S*)-absolute configuration of the major diastereomeric complex and the (*S*)-absolute configuration of the isolated amino acid was established.

2.2. C-alkylation of α-H amino acid fragment of the intermediate complex

To a solution of Ni^{II}-(*S*)-BPB-(*S*)-PGly (0.5 g, 0.0009 mol) in 10 mL of DMF, 0.216 mL (0.0014 mol) of 4-(trifluoromethyl)benzyl bromide and 0.11 g (0.0028 mol) of NaOH were added under stirring

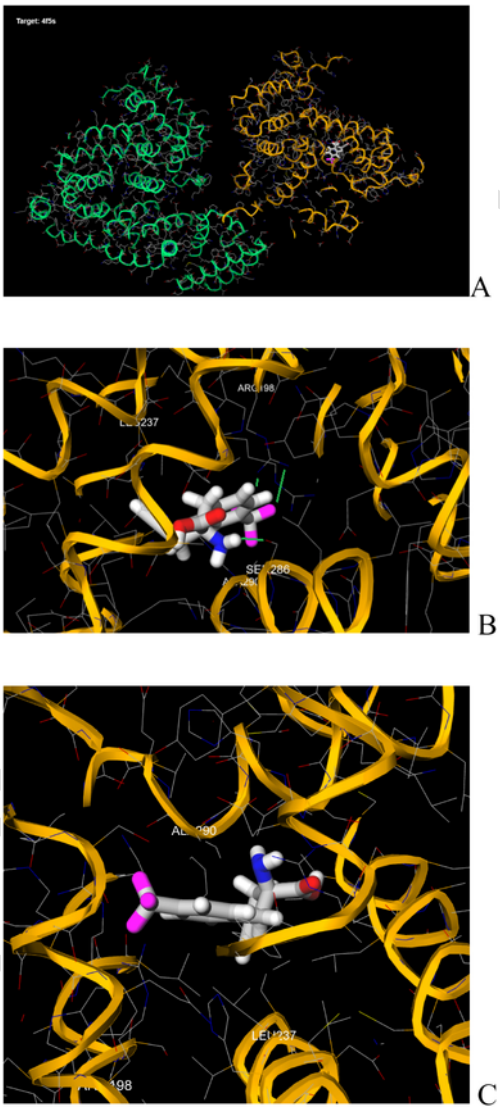

Fig. 7. The docked structure of the CFIIIPhe/BSA complex (A) with details of ligand-interacting residues (B,C).

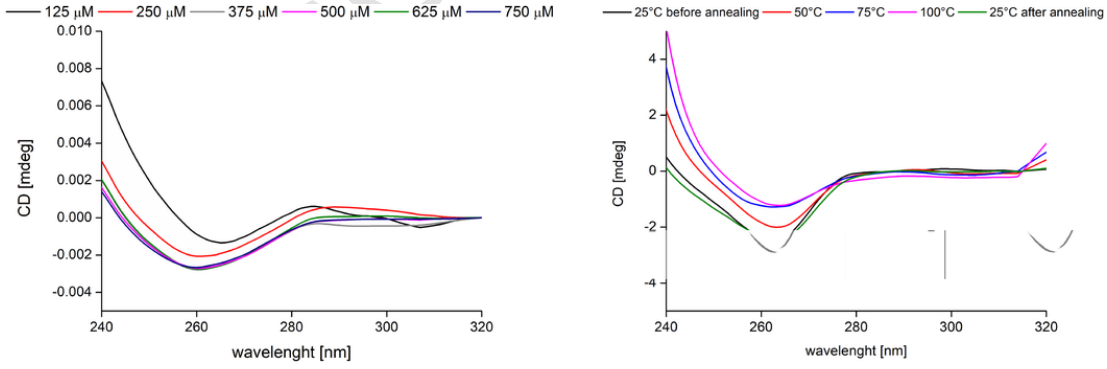

Fig. 8. CD aggregation studies relative to CF3IIIPhe at different concentrations (in the 0.125–0.75 mM range) in 1 × PBS buffer (pH 7.4) at 25 °C. All CD spectra were normalized for concentration (A); CD spectra of CF3IIIPhe at different temperatures (in the 25–100 °C range) in 1 × PBS buffer (pH 7.4) at the concentration of 0.75 mM (B).

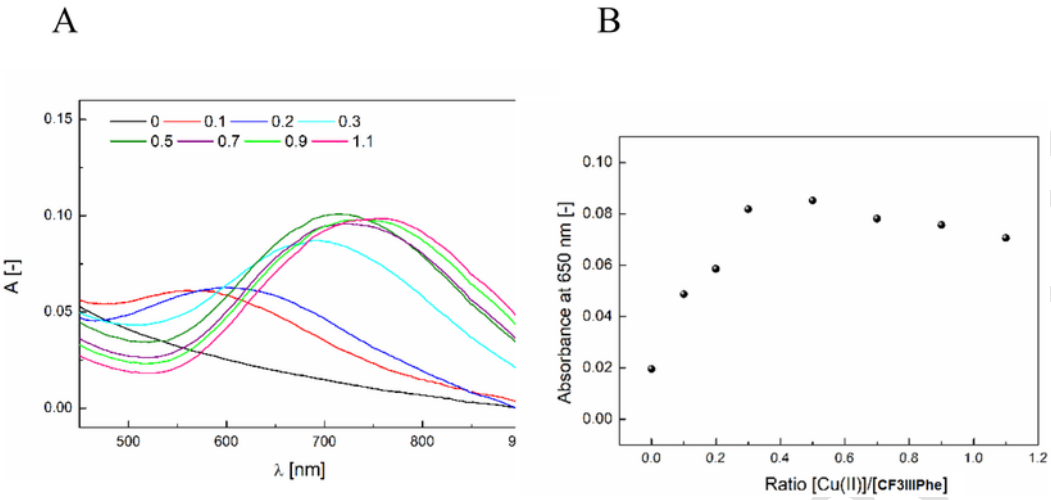

Fig. 9. UV–Vis Cu(II)-binding studies on CF3IIIPhe in methanol: spectrophotometric titration curves of CF3IIIPhe (A) with Cu(II); plots of absorbance at 650 nm vs concentration ratio, [Cu(II)]/[CF3IIIPhe] (B).

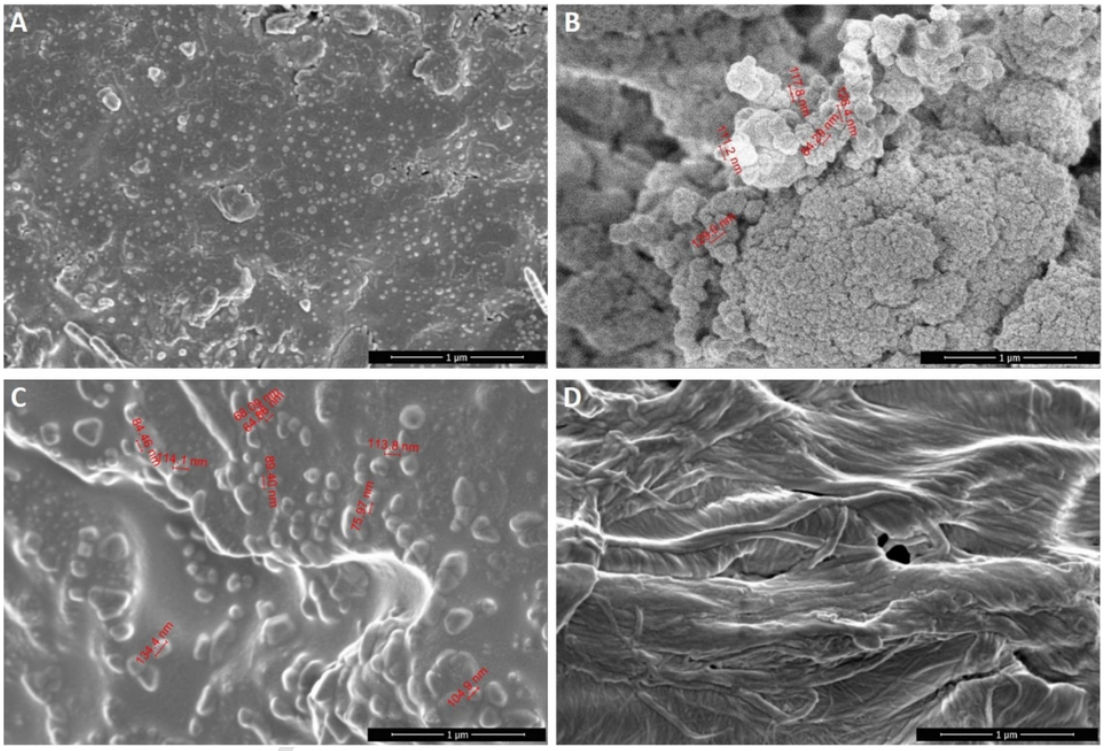

Fig. 10. SEM analysis of tel_{26} DNA/CF3IIIPhe complex: Micrographs at 100,000× (1 μm) of CF3IIIPhe (A); tel_{26} DNA (B); two different regions of (CF3IIIPhe + tel_{26} DNA) sample (C and D) in 10 mM TrisHCl, 100 mM KCl, pH 7.4; C_{DNA} = 2.5 μM $C_{CF3IIIPhe}$ = 125 μM.

at 25 °C. The reaction was monitored by TLC (SiO_2, $CHCl_3$/ethylacetate = 1:3) following the disappearance of the spot of the initial complex. Upon completion of the reaction, the mixture was precipitated by H_2O and the product was crystallized from methanol (75% yield).

Anal. Calc. for $C_{38}H_{32}F_3N_3NiO_3$ (694.37): C, 65.73; H, 4.65; N, 6.05; Found: C 65.78; H 4.69; N 6.13. Mp. 179 °C. $[\alpha]_D^{20}$ = +2′070.0° (c 0.15, CH_3OH). ^{1}H NMR - ($CDCl_3$ d, m.d., *Hz*): δ = 1.47–1.60 m (1H) & 1.61–1.73 m (1H, γ-CH_2 Pro); 1.80 td (1H, *J* 10.4, 6.2, δ-H_a Pro); 1.99–2.13 m (1H, β-Ha Pro); 2.11 dd (1H, *J* 17.4, 2.5, CH(H) C≡CH.); 2.20–2.34 m (1H, β-H_b Pro); 2.43 t (1H, *J* 2.5, ≡CH); 2.76 d (1H, *J* 13.6, CH_2-Ar.); 2.91 dd (1H, *J* 17.4, 2.5,CH(H) C≡CH); 2.99–3.07 m (1H, δ-H_b Pro); 3.11 d (1H, *J* 13.6, CH_2-Ar.); 3.20 dd (1H, *J* 10.3, 6.5, α-H Pro); 3.27 d (1H, *J* 12.4) & 4.25 d (1H, *J* 12.4, CH_2-Ph); 6.55 dd (1H, *J* 8.5, 2.0, H^3 C_6H_4); 6.59 ddd (1H, *J* 8.5, 6.6, 1.2, H^4 C_6H_4); 7.07 ddd (1H, *J* 8.6, 6.6, 2.0, H^5 C_6H_4); 7.09 tt (1H, *J* 7.4, 1.2, H^4 Ph);7.20–7.31 m (3H); 7.42–7.48 m (1H); 7.54–7.62 m (4H); 7.75–7.80 m (2H); 7.95–7.99 m (1H); 7.99 dd (1H, *J* 8.6, 1.2, H^6 C_6H_4); 8.28–8.33 m (2H, m, $H^{2,6}$ Ph). ^{13}C NMR (75.5 MHz, $CDCl_3$): δ = 22.6 (γ-CH_2 Pro); 30.7 (β-CH_2 Pro); 31.9 (CH_2 C≡CH); 43.2 (CH_2-Ar.); 58.3 (δ-CH_2 Pro); 64.7 (CH_2Ph); 70.6 (α-CH Pro); 73.2 (≡CH); 80.0 (C-CH_2Ar.); 80.6 (≡C); 120.5 (C^4H C_6H_4); 123.8 (C^6H C_6H_4); 124.3 q ($J_{C,F}$ 272.2,

CF_3); 125.8 q ($J_{C,F}$ 3.6, $C^{2,6}H$ $C_6H_4CF_3$); 127.6; 127.7 (CH); 127.9 (CH); 128.1 (CH); 128.9 (2CH); 129.1129.6 (CH); 130.1 (CH); 130.3 (q, $J_{C,F}$ 33.0, $\underline{C}CF_3$); 131.4 (2CH); 131.5 (2CH); 132.0 (CH); 133.8 (CH); 134.5; 136.8; 140.5; 142.7; 173.1; 178.9; 180.6.

2.3. Isolation of the amino acid

Complex was dissolved in 50 ml of MeOH and then slowly added to 50 ml of 2 M HCl solution and the mixture was heated at 50 °C. After disappearance of the red color of the metal complex, the solution was concentrated in vacuum, then 50 mL of water was added and the precipitated (*S*)-BPB × HCl was filtered. The optically active amino acid was isolated from the water layer by ion-exchange sorption and desorption using Ku-2 × $8H^+$ for cation exchange and an aq. solution of NH_4OH (5%) as eluent. The eluate was concentrated in vacuum and the amino acid was recrystallized from a mixture of water and EtOH (1:2). The compound was isolated in the analytically pure form.

2.3.1. (S)-2-amino-2-(4-(trifluoromethyl)benzyl)pent-4-ynoic acid (CF3IIIPhe)

Yield 86,67%. Anal. calc. for $C_{13}H_{12}F_3NO_2$ (271.24) C 57.57; H 4.46; N 5.11. Found: C 57.55; H 4.48; N 5.00. M.p. 241 °C (decomposed and became black), $[\alpha]_D^{20} = +18.5$ (c 0,2, 6 N HCl). ^1H NMR (DMSO –d6/CCl_4 + CF_3COOD, Hz): δ =2.55 (1H, t, *J* 2.5, ≡CH); 2.72 (1H, dd, *J* 17.5, 2.5) & 2.87 (1H, dd, *J* 17.5, 2.5, $CH_2C{\equiv}CH$); 3.14 (1H, d, *J* 14.1) and 3.33 (1H, d, *J* 14.1, $CH_2C_6H_4CF_3$); 7.36–7.41 (2H, m) and 7.62–7.67 (2H, m, $C_6H_4CF_3$). ^{13}C NMR (75.5 MHz, $CDCl_3$): δ=24.8 (CH_2); 39.5 (CH_2); 62.3; 74.8 (CH Acet.); 75.5 (C Acet.); 115.5 (q, *J*~285, CF_3); 125.4 (q, *J* 3.5, 2CH); 130.2 (2CH); 129.2 (q, *J* 30.0); 136.1; 170.6 (CO).

2.4. In silico pharmacokinetic properties prediction

The SMILES (Simplified Molecular Input Line Entry System) code of CF3IIIPhe was obtained with MOLVIEW (http://molview.org) software. The SMILES code was applied to calculate the physicochemical properties and lipophilicity, e.g. molecular weights (MW), the logP values (octanol-water partition coefficient), in six variants (ILOGPs, XLOGP3, WLOGP, MLOGP, SILICOS-IT and consensus logP (clogP) being an average of five mentioned predictions); tPSA (topological polar surface area), number of hydrogen-bond acceptors and donors, number of atoms, rotatable bonds, ring, carbon and heteroatoms. Calculations of pharmacokinetic profile descriptors of the synthesized compound were performed with various software packages, accessible on-line. The clogP values were calculated with SwissADME web service [22], ILOGPs with in-house physics-based method implemented from Daina A. et al. [23], XLOGP3 with atomistic and knowledge-based method calculated by XLOGP program, version 3.2.2, courtesy of CCBG, Shanghai Institute of Organic Chemistry, WLOGP with atomic method implemented from Wildman SA and Crippen GM [24], MLOGP with topological method implemented from Moriguchi I et al. [25] and Lipinski PA et al. [26], SILICOS-IT with hybrid fragmental/topological method calculated by FILTER-IT program, version 1.0.2, courtesy of SILICOS-IT, http://silicos-it.com, other not mentioned parameters with SwissADME web service [22]. Calculations of electrostatic potential in Fig. S2 were performed by Avogadro program [27].

2.5. Biological assays: materials, chemicals and cell lines

2.5.1. Chemicals

Thiazolyl blue tetrazolium bromide and 1-octanol were purchased from Sigma Aldrich, Phosphate Buffered Saline (PBS) form Gibco, cell counting Kit 8 (CCK-8) assay from Dojindo Lab, Japan.

2.5.2. Cell culture medias and supplements

DMEM medium, 10 mg/ml antibiotics (penicillin and streptomycin) were purchased from Sigma Aldrich, EMEM medium from ATCC, fetal bovine serum (FBS) and RPMI-1640 medium form Gibco, L-glutamine from Lonza.

2.5.3. Cell lines

Human glioblastoma T98G (ATCC® CRL-1690™), human lung carcinoma A549 (ATCC® CCL-185™), human breast adenocarcinoma MDA-MB-231 (ATCC® HTB-26™), human mammary gland T47D (ATCC® HTB-133™), human keratinocyte HaCaT (ATCC® PCS-200-011™) and human prostate cancer PC3 (ATCC® CRL-1435™) cells were purchased from ATCC (Manassas, USA).

2.6. Cell line culture conditions

Cell lines T98G were cultured in EMEM medium, HaCaT, A549 and MDA-MB-231 in DMEM medium, T47D and PC3 in RPMI-1640 medium. Each medium was supplemented with 10% (v/v) FBS and 10 mg/ml antibiotics (penicillin and streptomycin) and PC3 also with 1% L-glutamine. Cells were cultured at 37 °C with 5% CO_2 in humidified air.

Cells were seeded at 1×10^4 cells per well in 96-well plates containing 0.1 ml appropriate supplemented medium (HaCaT, T98G, MDA-MB-231, A547, T47D) or at 4×10^3 cells per well in 96-well flat-bottom plates containing 0.05 ml of medium (PC3). Cells with 85–95% confluence, after 24 h were washed with PBS, placed in fresh medium 0.1 ml and treated with increasing concentrations (0.025, 0.25, 2.5, 25, 250 μM) of CF3IIIPhe. The viability of cells was determined 24 and 48 h after cell culture supplementation with the studied compound.

2.7. Cell viability assay

Cell viability of HaCaT, T98G, MDA-MB-231, A547, T47D cells was evaluated with a dye-staining method, using 3-(4,5-dimethyl-2-thiazolyl)-2,5-diphenyl-2H-tetrazolium bromide (MTT) [28]. 24 and 48 h after treatment, the medium was removed and 0.1 ml of MTT solution in medium (0.5 mg/ml final concentration of MTT) was added to each well for 2 h. Then the cell supernatant was removed and the formazan crystals were dissolved in 0.1 ml/well DMSO, and measured spectrophotometrically in a multi-well Synergy2 plate reader (BioTek Instruments, USA) at a test wavelength of 492 nm and a reference wavelength of 690 nm. Cell viability of PC3 cells was evaluated with cell CCK-8 assay following the manufacturer instructions (Dojindo Lab, Japan). The assay was performed by adding 10 μl of the CCK-8 solution directly to culture wells and incubating for 2 h at 37 °C, in a 5% CO_2 humidified atmosphere. Finally, absorbance was measured at 450 nm using a microplate reader (Multiskan Fc 10094).

Calculations and data analysis were done using GraphPad Prism v5.01 (GraphPad Software, Inc., USA). Values represent the means from at least three independent experiments.

2.8. CD and UV studies

The CD spectra were obtained on a J-810 spectropolarimeter (Jasco Europe S.R.L., Cremella, Italy) equipped with a Peltier PTC-423S/15, using a Hellma (Milan, Italy) quartz cell (1 cm). In the investigation of tel_{26} and c-myc the spectra were measured in the 200–320 nm wavelength range at 20 °C, while in BSA measurements between 204 and 250 nm at 15 °C.

In all experiments, we used 2.5 μM of DNA (tel_{26}: $^{5'}$TTAGGGTTAGGGTTAGGGTTAGGGTT$^{3'}$ or c-myc: Pu22, $^{5'}$TGAGGGTGGGTAGGGTGGGTAA$^{3'}$, 1 equiv.; supplied by Genomed S.A., Poland) + 125 μM amino acid (50 equiv.) in 10 mM TrisHCl (10 mM TrisHCl, 100 mM KCl, pH 7.4) (tel_{26}) or 1 × PBS (pH 7.4; Sigma Aldrich) (c-myc) buffer (pH = 7.4) added with 100 mM KCl, annealed at 95 °C for 5 min and left overnight at room temperature to slowly cool down (16 h). CD melting of telomeric and c-myc G4 DNAs was obtained by recording CD values at 295 and 263 nm, respectively, as a function of temperature. Melting temperature values were determined as the temperatures relative to minima of the 1st derivative plots of denaturation curves. All experiments were repeated at least in duplicate and all spectra were recorded in triplicate till stabilization of the signals. Presented curves are average of two experiments.

For Bovine Serum Albumin (BSA; Sigma Aldrich) binding experiments we used the following conditions: 75 nM BSA + 250 equiv. of amino acid in PBS (pH 7.4). The results are expressed as MRE (mean residue ellipticity) in deg cm^2 dmol^{-1}, which is given by:

$$\mathrm{MRE} = \frac{observed\ CD\ (mdeg)}{C_p n l} \quad (1)$$

where C_p is the molar concentration of the protein, n is the number of amino acid residues (582) and l is the path length (1 cm). The α-helix content of free and bound BSA was calculated from the MRE value at 209 nm using the formula:

$$\alpha - \mathrm{helix}\% = \frac{\left[-MRE_{209} - 4000\right]}{\left[33000 - 4000\right]} \times 100 \quad (2)$$

where MRE_{209} is the observed value at 209 nm, 4000 is MRE of the β-sheet and random coil conformation at 209 nm, and 33,000 is the MRE value of pure α-form at 209 nm [29].

UV spectra were recorded on a Jasco V770 spectrophotometer equipped with a PAC-743R Automatic 6/8-Position Peltier Cell Changer.

2.9. Docking studies

The structure of BSA was obtained from the Protein Data Bank database [PDB; http://www.rcsb.org/pdb: 4F5S]. Molecular docking of CFIIIPhe with binding site I of BSA was performed using the AutoDock Vina docking algorithm employed in the program 1-Click Docking (Mcule Inc., Palo Alto, CA, USA). The binding site center was established as default, with the Cartesian coordinates (X: −6.152, Y: 24.872 and Z: 108.686), and the size of the binding site was 22 Angstrom. We selected the docking pose with the most negative docking score (−7.0 kcal/mol) corresponding to the highest binding affinity and H-bonding was analyzed by WebLab ViewerPro (Molecular Simulations Inc., San Diego, CA, USA).

2.10. Determination of experimental logP

logP value was determined following the procedure of Zhao et al. [30]. More in detail, we recorded the UV absorbance at λ_{max} (264 nm) of CF3IIIPhe (2 mg) dissolved in 5 mL in 1-octanol (A_0) and the absorbance (A_x) at the same wavelength recorded for the octanol phase after stirring the above solution in the presence of 5 mL of sodium phosphate buffer (pH 7.5) over 30 h. The found UV absorbance values were $A_0 = 0.192 \pm 0.006$ and $A_x = 0.178 \pm 0.003$. Afterwards, we calculated the octanol/water partition coefficient (logP = 1.1 ± 0.2) according to the following equation (3):

$$logP = \log \frac{A_x}{A_0 - A_x} \quad (3)$$

3. Results and discussion

3.1. Synthesis

First, the synthetic amino acid was obtained by a stereoselective approach that allows one to synthesize unsaturated α-amino acids in an optically active form. As starting amino acid synthon for the asymmetric synthesis of our amino acid, we used a Ni(II) square-planar complex of the Schiff's base formed by propargylglycine (PGly) with the chiral auxiliary (*S*)-2-N-(N′-benzyl-prolyl)aminobenzophenone (BPB) (Fig. 2). Such Ni (II) complex, indicated as Ni(II)-(*S*)-BPB-(*S*)-PGly, was synthesized according to literature procedures [21].

Successively, we performed the C-alkylation of the amino acid α-position of the complex (Scheme 1) with the formation of the desired α-substituted propargylglycine analogue. The asymmetric C-alkylation of this derivative led to the 4-(trifluoromethyl)benzyl derivative with satisfying diastereoselectivity (Scheme 1).

We found as optimized conditions for this reaction the usage of DMF as a solvent, a temperature of 25 °C, as well as a 1/3/1.5 equivalent ratio of the complex/NaOH/alkylating agent system. The reaction was monitored by TLC (silica gel) using a $CHCl_3$/EtOAc = 1:3 eluent system. We noticed, besides the predominant expected products, the formation of a significant amount of undesired by-products (up to 10%). The diastereomeric excess (*de*) of the complexes was determined by ^{1}H NMR spectroscopy by analysis of the integrals of the doublet signals assigned to the methylene protons of the N-benzyl group of the BPB fragment for both diastereomers. The *de* value (74.5%) of the complex was also confirmed by HPLC analysis of the final amino acid (before chromatography). The major diastereomer of the complex was isolated by crystallization from methanol, while the absolute configuration of the amino acid moieties present in the complex was determined by measuring the specific rotation at 589 nm, as previously reported for other similar complexes of amino acids based on the chiral auxiliary (*S*)-BPB.

The subsequent step was the complex hydrolysis with aqueous HCl, followed by recovery of the insoluble hydrochloride of the (*S*)-BPB and purification of the amino acid CF3IIIPhe by an ion-exchange method and crystallization from a mixture of water and ethanol (1:1), that afforded the desired amino acids with high enantiomeric purity (ee >97%, Scheme 2).

3.2. Computational studies

To gain information on the druglikeness of the novel synthetic aromatic alkyne-containing amino acid we performed preliminary computational studies whose results are summarized in Table S1. The most common criteria used for the prediction of druglikeness for a given molecule encompass the Lipinski's rules [31], according to which an active drug should have [23] a molecular weight lower than 500 Da, five (or less) hydrogen bond donors, no more than ten hydrogen bond acceptors, and a calculated logP (octanol-water partition coefficient) lower than 5 [31].

Physicochemical properties and lipophilicity of CF3IIIPhe were determined (Table S1). This compound clearly fulfills the Lipinski's rules. Furthermore, we showed that it fulfills also criteria of druglikeness implemented by others, i.e. Ghose AK et al. [32], Veber DF et al. [33], Egan WJ et al. [34] and Muegge I et al. [35] (Table S1). Physicochemical properties and lipophilicity of our new synthetic aromatic amino acid makes it a promising drug candidate. Calculated topological polar surface area (tPSA) for the tested compound is 63.32 $Å^2$, which indicates its efficient transport through the membranes. Therefore, as tPSA value calculated is lower than 65 $Å^2$, CF3IIIPhe is potentially able to cross the blood-brain barrier. The analyzed structure fulfills also a criterion of aromaticity which is extremely important for bioavailability and drug-target interaction via van der Waals forces or π-stacking. In fact, more than two aromatic rings reduce the drug hydrophilicity and may lead to a poor drug distribution within the body [36]. In order to compare the predicted (clogP, Table S1) and experimental logP, we performed a solvent extraction experiment on CFIII-I3Phe with a 1-octanol/aqueous solution mixture following the procedure of Zhao et al. [30] and determined the logP by Eq. (3) as 1.1 ± 0.2, which is in a good agreement with the predicted value (clogP = 0.96, Table S1).

3.3. Cells viability studies

Aiming at exploring the anticancer potential of the synthetic amino acids, we evaluated its cytotoxicity towards a panel of cancer cells in comparison to nontumorigenic control ones. Thus, the effect of CF3IIIPhe on cell viability was assayed on cancerous (T98G, MDA-MB-231, A549, T47D, PC3) and non-cancerous (HaCaT) cell lines (Fig. 3). We found a significant effect of our synthetic amino acid on PC3 cells as observed after 24 h in the tested range of concentrations (0–250 μM, Fig. 3). Excluding PC3 cell line, the effect of the compound on viability of the other cancer cells (lower, anyway, than that seen on prostate cancer cells) is more meaningful after 48 h as seen on T98G, confirming the anticancer potential of this compound (Fig. S3). It is important to underline that CFIIIPhe was not toxic to nontumorigenic cells as we ascertained with HaCaT cell line (Figs. 3 and S3). From a quantitative perspective, the cell viability of PC3 cells treated with CF3IIIPhe, after 24 h treatment was 31% lower than untreated cells. No additional cell proliferation decrease was seen after 48 h. Interestingly, we observed a good antiproliferative activity at 24 h on PC3 cells with an EC_{50} of 143 nM, whereas cisplatin in the same conditions showed a 10 μM EC50 (Fig. S4).

Nevertheless, the comparison of the total inhibition effects (revealing an overall higher antiproliferative effect of cisplatin) and the different shapes for the dose-response curves suggest different anticancer mechanisms in the two cases. Additionally, the unnatural amino acid decreased cell viability of T98G cells after 48 h with a 29% reduction of cell proliferation observed in this case after treatment with 250 μM CF3IIIPhe (Fig. S3).

3.4. Interaction with telomeric DNA and the c-myc oncogene promoter

In order to shed light on the possible mechanisms underlying the observed anticancer activity of CF3IIIPhe, its potential in binding telomeric DNA (using the 26-base tract tel_{26}) and c-myc was evaluated. In general, telomeric DNA adopts hybrid-1, hybrid-2, and antiparallel basket topologies [37]. In particular, in our experiments we observed a CD spectrum corresponding to a hybrid-type topology (Fig. 4) with a characteristic positive peak at 290 nm, a shoulder peak at 270 nm and a small negative peak at 240 nm. On other side, c-myc adopts a parallel topology indicated by a CD profile with a positive peak at 260 nm and a negative one at 240 nm (Fig. 5) [38].

As shown in Fig. 4A the synthetic amino acid induces only slight changes to telomeric DNA CD spectrum. This suggests that CF3II-IPhe does not alter significantly the secondary G4-DNA structure. CD melting experiments (Fig. 4B and C) revealed a slight enhancement of telomeric DNA thermal stability by CF3IIIPhe.

In particular, CF3IIIPhe interaction afforded a DNA stabilization with a T_m increased by ~1.5 °C (Table 1). In this regard, telomeric DNA stabilization is an important goal for anticancer drugs and a well recognized feature in the interpretation of their biological anticancer mechanism [11].

We performed analogous studies also on c-myc oncogene promoter DNA finding again a slight modification of nucleic secondary structure of the parallel G4 DNA topology by the investigated compound that, strikingly, led in this case to the destabilization effect (by ~3.5 °C) of the c-myc quadruplex DNA (Fig. 5 and Table 2). Overall, our CD investigation suggests that CF3IIIPhe does not alter the core secondary structure of the two G4 systems. Hence, we exclude any ability of the compound to stack on the G-quartets and suggest a higher propensity of CF3IIIPhe to interact with the G4 by forming hydrogen bonds and hydrophobic interactions with G4 loops and/or grooves.

Moreover, the fact that CF3IIIPhe caused opposite thermal stability changes in tel_{26} and c-myc DNAs, seems to indicate its ability to interact differently with mixed parallel/antiparallel compared to parallel G4 systems.

This different behavior of our unnatural amino acid with the two G4 systems explored, clearly reflects the structural diversity in the relative topologies and is in accord with other previous reports of aromatic ligands behaving differently with either parallel (c-myc) or mixed parallel/antiparallel (telomeric) DNA topologies [39].

3.5. Interaction of synthetic compounds with a model protein

To explore the ability of CF3IIIPhe to interact with the family of proteins we used BSA (bovine serum albumin) as a protein model system. The CD spectrum of BSA exhibits two negative bands (λ = 209 nm and 222 nm) arising from the typical α-helix structure of protein (Fig. 6) [40]. A variation of the CD doublet peak intensity indicates a change in the α-helical secondary structure content that can be observed upon ligand/protein binding [41]. The CD profiles at 15 °C of BSA in the presence and absence of CF3IIIPhe are shown in Fig. 6. The α-helix content of the protein, calculated according to the Eqs. (1) and (2) (see Experimental), was 54.2% which is in reasonable relation to the literature [42]. Remarkably, CF3IIIPhe showed a clear binding efficacy towards the model protein and decreased the α-helix content to 47.6%. Apart from its utility as protein model system, serum albumin binding has also an intrinsic importance as it influences the effective availability of a drug in cells, with free un-

bound concentration of the drug determining its therapeutic potential [43].

3.6. Molecular docking

We evaluated in silico the docking of CFIIIPHE to the drug binding site I of subdomain IIA (domain II) of BSA, the main ligand binding region of plasma proteins, in analogy to previous literature reports on other CF_3-modified aromatic BSA ligands [44].

We found that CF3IIIPhe bound the drug binding site I of BSA, with a free binding energy of −7.0 kcal/mol, and was embedded into a protein cavity (Fig. 7) in which hydrophobic (Leu-237, Leu-241, Leu-259, Ile-263, Ala-290, Trp-213), polar (Ser-286), and charged amino acids (Arg-194, Arg-198, Arg-217) surrounded the ligand. More in detail, Leu-237 and Ala-290 gave hydrophobic interactions with the apolar moiety of the compound, while the amino acid residues Arg-198 and Ser-286 were involved in hydrogen bonding between CFIIIPhe and BSA. In fact, Ser-286 accepted H-bond from CFIIIPhe amino group (H-bond length: 2.11 Å), while CF_3 acted as an H-bond acceptor for the guanidinium group of arginine 198 (H-bond length: 2.44 Å) [45].

3.7. Aggregation evidences

The aggregation propensity is one of the aspects to be evaluated in a potential drug, as aggregate appearance inside or in the space surrounding cancer cells was found responsible for the anticancer activity of several drugs described previously [46].

Aiming at exploring aggregate formation CD spectra were recorded at 25 °C for the unnatural amino acid in aqueous solution. The signal was very weak but the spectral intensity increased with concentration, and by normalizing the spectra for concentration, we noticed concentration-dependent CD changes for CF3IIIPhe (Fig. 8A) that suggested its ability to aggregate forming non-covalent polymeric systems under the experimental conditions employed.

CF3IIIPhe showed also a temperature-dependent behavior (Fig. 8B) that confirmed the above hypothesis. More in particular, CD signal intensity decreased as effect of heating, as expected for a thermal disaggregation of the noncovalent polymers. The process is reversible, as the CD spectrum at 25 °C, obtained after the heating and the successive cooling steps, is pratically superimposable to that recorded initially at 25 °C reflecting the restoration of the aggregate structure.

3.8. Copper(II) binding

Cu(II) chelating agents were found to be able to deprive cancer cells of this important metal ion provoking anticancer effects [47]. Thus, we were interested in investigating whether our synthetic amino acid was able to act as a Cu(II) binder, which could be an useful property concurring with the anticancer potential of our derivative. Cu(II) binding ability was studied by UV–Vis spectroscopy according to other literature reports on compounds that, similarly to our compound, had a certain tendency to aggregate/precipitate from aqueous solutions and that were studied, thus, in organic solutions.

By studying the absorbance variations of the typical copper band at 600 nm as a consequence of the progressive adds of derivative amounts, we observed that CF3IIIPhe was able to bind Cu(II) cation causing the spectroscopic variations shown in Fig. 9. By titration curve analysis (Fig. 9) a certain stabilization of absorption signal was observed for CF3IIIPhe at a ratio value ~0.5. This suggests that the unnatural amino acid forms complexes with a 2:1 ligand to metal ratio.

3.9. SEM microscopy

Scanning electron microscopy was applied to the analysis of morphologies adopted by telomeric DNA tel_{26} and its complex with the anticancer CF3IIIPhe. SEM images of dried samples, shown in the micrographs of Fig. 10, present a surface morphology for CF3IIIPhe with a quite homogenous film visible at low magnifications (Fig. 10A), that at higher magnifications revealed numerous spherical structures (with widths of 30–50 nm). On the other side, the sample of tel_{26} DNA contains several roughly micrometric sized aggregates consisting of nanospheres (with widths ~80–130 nm or smaller, Fig. 10B). The sample with the tel_{26}/CF3IIIPhe complex shows, instead, a structure differing significantly, both in morphology and size of the observed aggregates, from that of the unbound DNA. Indeed, fibers of micrometric length and thickness with a double superficial morphology, are clearly visible for the complex: fibers with several nanospheres (~50–100 nm sized or smaller, Fig. 10C) on their surfaces, as well as bundles of nanofibrils (with widths ~20–50 nm and lower) with a preferential orientation (Fig. 10D).

Similar nanofibrillar and nanospherical structures are reported in literature [48] for other nucleic acid-containing systems, in which, however, the nanofibrils are smaller (10–20 nm) and the nanospheres larger (160–200 nm width) than those observed in this study. Overall, the different morphologies found for the samples obtained mixing CF3IIIPhe with DNA, and unbound DNA support the already reported hypothesis of interaction of this unnatural amino acid and telomeric DNA.

4. Conclusion

In conclusion, in this work, we evaluated by spectroscopy the ability of a non-proteinogenic amino acid to bind G4 DNAs, a serum protein and copper (II) ions. Pharmacokinetic properties of CFIIIPhe determined in silico indicated it a promising drug candidate. Among these, the octanol/water partition coefficient (logP), one of the most important parameters in the assessment of druglikeness of a drug candidate, was determined also experimentally and compared with the predicted result showing good agreement (experimental $logP = 1.1 \pm 0.2$ vs. $clogP = 0.96$). Nevertheless, the biological effects of CFIIIPhe observed in various cell lines confirmed the efficient compound transport through the cell membranes.

CD and UV studies revealed that CF3IIIPhe: i) interacted with G4 DNAs without altering the core structures of the antiparallel/parallel (tel_{26}) and parallel (c-myc) G4 topologies, and slightly stabilizing only the former structure, ii) bound Cu(II) cation, and iii) formed aggregates in aqueous solution. Moreover, CF3IIIPhe was able to bind proteins, as we observed by CD with BSA, used as a model protein. Molecular docking studies demonstrated that the binding site I in subdomain IIA hydrophobic region of BSA could house CFIIIPhe in analogy to other literature reports on similar BSA ligands [44]. Its anticancer potential was also evaluated in cellular studies performed on a panel of human cancer cells in comparison with non-cancerous ones. We found that compound CF3IIIPhe lowered cell proliferation in PC3 cancer cells by 31% after 24 h of treatment without any undesired toxicity on nontumorigenic cells. Overall, the evidences emerged from this investigation suggested that CF3IIIPhe may exert its anticancer activity as a consequence of a combination of factors, including possibly its ability to bind (as evidenced by CD and SEM) telomeric DNA. Besides these encouraging results, in consideration

of the seemingly unlimited functional versatility of unnatural amino acids, we propose our derivative as chiral building block and molecular scaffold in constructing peptidic or non-peptidic drugs to be investigated in future biomedical applications.

Author contributions

M.A.F. and A.F.M. performed most of the experiments and contributed to the manuscript preparation; G.N.R. performed the study design, performed CD melting experiments and worked on manuscript preparation; A. S. S., L. A. H., and H. S. performed synthesis of CF3I-IIPhe and took part in data analysis; R.P. and A.B. performed the biological studies and gave an important contribution to the manuscript preparation. V.R. performed SEM experiments and data analysis.

Declaration of competing interest

There are no conflicts to declare.

Acknowledgements

We are grateful to Dr. Wei Peng, Ph.D. (Xiamen University, China) and Mr. Gergely Takács (Mcule team, Hungary) for their kind support in molecular docking studies, and Dr. Viviana De Rosa (IBB CNR) for useful discussion. We also would like to thank Dr. Flavia Squeglia (IBB CNR) and Mr. Miguel Moreira (IBB CNR) for their precious suggestions in manuscript preparation. We thank Ministero dell'Istruzione, dell'Universita' e della Ricerca (MIUR), Italy [grant number PON03PE 00060 4 and MERIT prot. RBNE08YFN3_009] and to the National Science Centre, Poland [grants SONATINA no. 2017/24/C/ST5/00181 and UMO-2018/28/C/NZ1/00497].

Appendix A. Supplementary data

Supplementary data, including computer assisted studies on the unnatural amino acid, with chemical properties, energy-minimized structures, electronic potential surfaces, HPLC and NMR characterization data, as well as cellular assays are reported. Supplementary data to this article can be found online at https://doi.org/10.1016/j.saa.2019.117884.

References

[1] W. Ko, S. Kim, K. Jo, H.S. Lee, Genetic incorporation of recycled unnatural amino acids, Amino Acids 48 (2016) 357–363.
[2] S. La Manna, L. Lopez-Sanz, M. Leone, P. Brandi, P.L. Scognamiglio, G. Morelli, E. Novellino, C. Gomez-Guerrero, D. Marasco, Structure-activity studies of peptidomimetics based on kinase-inhibitory region of suppressors of cytokine signaling 1, Biopolymers 110 (2018) e23082.
[3] A. Carotenuto, L. Auriemma, F. Merlino, A.M. Yousif, D. Marasco, A. Limatola, P. Campiglia, I. Gomez-Monterrey, P. Santicioli, S. Meini, C.A. Maggi, E. Novellino, P. Grieco, Lead optimization of P5U and urantide: discovery of novel potent ligands at the urotensin-II receptor, J. Med. Chem. 57 (2014) 5965–5974.
[4] F. Zarrilli, F. Amato, C.M. Morgillo, B. Pinto, G. Santarpia, N. Borbone, S. D'Errico, B. Catalanotti, G. Piccialli, G. Castaldo, G. Oliviero, Peptide nucleic acids as miRNA target protectors for the treatment of cystic fibrosis, Molecules 22 (2017) 1144.
[5] G.N. Roviello, C. Vicidomini, S. Di Gaetano, D. Capasso, D. Musumeci, V. Roviello, Solid phase synthesis and RNA-binding activity of an arginine-containing nucleopeptide, RSC Adv. 6 (2016) 14140–14148.
[6] M.Y. Lidak, I.Z. Lulle, M.G. Plata, R.A. Paégle, V.É. Krishane, Peptides of aminonucleic acids, Chem. Heterocycl. Compd. 11 (1975) 1326–1329.
[7] G.N. Roviello, R. Iannitti, R. Palumbo, H. Simonyan, C. Vicidomini, V. Roviello, Lac-l-TTA, a novel lactose-based amino acid–sugar conjugate for anti-metastatic applications, Amino Acids 49 (2017) 1347–1353.
[8] G.N. Roviello, R. Iannitti, V. Roviello, R. Palumbo, H. Simonyan, C. Vicidomini, Synthesis and biological evaluation of a novel Amadori compound, Amino Acids 49 (2017) 327–335.
[9] A.S. Saghyan, H.M. Simonyan, S.G. Petrosyan, A.V. Geolchanyan, G.N. Roviello, D. Musumeci, V. Roviello, Thiophenyl-substituted triazolyl-thione l-alanine: asymmetric synthesis, aggregation and biological properties, Amino Acids 46 (2014) 2325–2332.
[10] D.M. Rasadean, B. Sheng, J. Dash, G.D. Pantos, Amino-acid-derived naphthalenediimides as versatile G-quadruplex binders, Chemistry 23 (2017) 8491–8499.
[11] G. Cimino-Reale, N. Zaffaroni, M. Folini, Emerging role of G-quadruplex DNA as target in anticancer therapy, Curr. Pharm. Des. 22 (2016) 6612–6624.
[12] A. Avino, C. Fabrega, M. Tintore, R. Eritja, Thrombin binding aptamer, more than a simple aptamer: chemically modified derivatives and biomedical applications, Curr. Pharm. Des. 18 (2012) 2036–2047.
[13] A.H. Romero, Role of trifluoromethyl substitution in design of antimalarial quinolones: a comprehensive review, Top. Curr. Chem. 377 (2019) https://doi.org/10.1007/s41061-019-0234-7.
[14] H.-X. Jiang, D.-M. Zhuang, Y. Huang, X.-X. Cao, J.-H. Yao, J.-Y. Li, J.-Y. Wang, C. Zhang, B. Jiang, Design, synthesis, and biological evaluation of novel trifluoromethyl indoles as potent HIV-1 NNRTIs with an improved drug resistance profile, Org. Biomol. Chem. 12 (2014) 3446–3458.
[15] L. Gregory, P. Armen, R.L. Frederic, Trifluoromethyl ethers and –thioethers as tools for medicinal chemistry and drug discovery, Curr. Top. Med. Chem. 14 (2014) 941–951.
[16] A. Burriss, A.J. Edmunds, D. Emery, R.G. Hall, O. Jacob, J. Schaetzer, The importance of trifluoromethyl pyridines in crop protection, Pest Manag. Sci. 74 (2018) 1228–1238.
[17] J.A. Marchand, M.E. Neugebauer, M.C. Ing, C.I. Lin, J.G. Pelton, M.C.Y. Chang, Discovery of a pathway for terminal-alkyne amino acid biosynthesis, Nature 567 (2019) 420–424.
[18] A. Siddiq, V. Dembitsky, Acetylenic anticancer agents, Anti Cancer Agents Med. Chem. 8 (2008) 132–170.
[19] C.J. Connelly, M.A. Strong, S.S. Lee, C.W. Greider, A.M. Pike, S. Wang, BRD4 inhibitors block telomere elongation, Nucleic Acids Res. 45 (2017) 8403–8410.
[20] B.-J. Chen, Y.-L. Wu, Y. Tanaka, W. Zhang, Small molecules targeting c-Myc oncogene: promising anti-cancer therapeutics, Int. J. Biol. Sci. 10 (2014) 1084–1096.
[21] S. Collet, P. Bauchat, R. Danion-Bougot, D. Danion, Stereoselective, non-racemic synthesis of ω-borono-α-amino acids, Tetrahedron-Asymmetr 9 (1998) 2121–2131.
[22] A. Daina, O. Michielin, V. Zoete, SwissADME: a free web tool to evaluate pharmacokinetics, drug-likeness and medicinal chemistry friendliness of small molecules, Sci. Rep. 7 (2017) 42717.
[23] A. Daina, O. Michielin, V. Zoete, iLOGP: a simple, robust, and efficient description of n-octanol/water partition coefficient for drug design using the GB/SA approach, J. Chem. Inf. Model. 54 (2014) 3284–3301.
[24] S.A. Wildman, G.M. Crippen, Prediction of physicochemical parameters by atomic contributions, J. Chem. Inf. Comput. Sci. 39 (1999) 868–873.
[25] K.K. Kawashima Y, Kato M., Hasegawa M., Tomisawa K., Hatayama K., Hirono S., Moriguchi I., Structure-activity studies of 3-benzoylpropionic acid derivatives suppressing adjuvant arthritis, Chem. Pharm. Bull., 40 (1992) 774–777.
[26] C.A. Lipinski, F. Lombardo, B.W. Dominy, P.J. Feeney, Experimental and computational approaches to estimate solubility and permeability in drug discovery and development settings1PII of original article: S0169-409X(96)00423-1. The article was originally published in Advanced Drug Delivery Reviews 23 (1997) 3–25.1, Adv. Drug Deliv. Rev. 46 (2001) 3–26.
[27] M.D. Hanwell, D.E. Curtis, D.C. Lonie, T. Vandermeersch, E. Zurek, G.R. Hutchison, Avogadro: an advanced semantic chemical editor, visualization, and analysis platform, J. Cheminform. 4 (2012) 17.
[28] C.P.R. Xavier, C.F. Lima, M. Rohde, C. Pereira-Wilson, Quercetin enhances 5-fluorouracil-induced apoptosis in MSI colorectal cancer cells through p53 modulation, Cancer Chemother. Pharmacol. (2011) 1449–1457.
[29] M. Mathew, S. Sreedhanya, P. Manoj, C.T. Aravindakumar, U.K. Aravind, Exploring the interaction of bisphenol-S with serum albumins: a better or worse alternative for bisphenol A?, J. Phys. Chem. B 118 (2014) 3832–3843.
[30] A. Zhao, Y. Li, C.M. Orahoske, B. Schnur, A. Sabbagh, W. Zhang, B. Li, B. Su, Lead optimization of selective tubulin inhibitors as anti-trypanosomal agents, Bioorg. Med. Chem. 27 (2019) 1517–1528.
[31] C.A. Lipinski, Drug-like properties and the causes of poor solubility and poor permeability, J. Pharmacol. Toxicol. Methods 44 (2000) 235–249.
[32] A.K. Ghose, V.N. Viswanadhan, J.J. Wendoloski, A knowledge-based approach in designing combinatorial or medicinal chemistry libraries for drug discovery. 1. A qualitative and quantitative characterization of known drug databases, J. Comb. Chem. 1 (1999) 55–68.

[33] D.F. Veber, S.R. Johnson, H.-Y. Cheng, B.R. Smith, K.W. Ward, K.D. Kopple, Molecular properties that influence the oral bioavailability of drug candidates, J. Med. Chem. 45 (2002) 2615–2623.
[34] W.J. Egan, K.M. Merz, J.J. Baldwin, Prediction of drug absorption using multivariate statistics, J. Med. Chem. 43 (2000) 3867–3877.
[35] I. Muegge, S.L. Heald, D. Brittelli, Simple selection criteria for drug-like chemical matter, J. Med. Chem. 44 (2001) 1841–1846.
[36] B.R. Prashantha Kumar, M. Soni, U. Bharvi Bhikhalal, I.R. Kakkot, M. Jagadeesh, P. Bommu, M.J. Nanjan, Analysis of physicochemical properties for drugs from nature, Med. Chem. Res. (2009) 984–992.
[37] A. Ambrus, D. Chen, J. Dai, T. Bialis, R.A. Jones, D. Yang, Human telomeric sequence forms a hybrid-type intramolecular G-quadruplex structure with mixed parallel/antiparallel strands in potassium solution, Nucleic Acids Res. 34 (2006) 2723–2735.
[38] K.V. Diveshkumar, S. Sakrikar, F. Rosu, S. Harikrishna, V. Gabelica, P.I. Pradeepkumar, Specific stabilization of c-MYC and c-KIT G-quadruplex DNA structures by indolylmethyleneindanone scaffolds, Biochemistry 55 (2016) 3571–3585.
[39] J. Medeiros-Silva, A. Guédin, G.F. Salgado, J.-L. Mergny, J.A. Queiroz, E.J. Cabrita, C. Cruz, Phenanthroline-bis-oxazole ligands for binding and stabilization of G-quadruplexes, BBA-Gen. Subjects 1861 ((2017) 1281–1292.
[40] J.-Q. Lu, F. Jin, T.-Q. Sun, X.-W. Zhou, Multi-spectroscopic study on interaction of bovine serum albumin with lomefloxacin–copper(II) complex, Int. J. Biol. Macromol. 40 (2007) 299–304.
[41] Z. Chen, S. Zhang, Z. Zhu, Y. Zhang, A novel platinum(ii) anticancer complex of danysl bis(2-benzothiazolylmethyl)amine with dimethyl sulfoxide as a leaving group: synthesis, cytotoxicity, interaction with DNA and human serum albumin, New J. Chem. 41 (2017) 6340–6348.
[42] S. Parveen, G. Velmurugan, E. Sinn, P. Venuvanalingam, S. Govindarajan, Water-soluble cobalt(II) & cobalt(III) complexes supported by new triazine Schiff base ligands: synthesis, structure and biological evaluation, J. Photochem. Photobiol. B 189 (2018) 152–164.
[43] D. Gonzalez, S. Schmidt, H. Derendorf, Importance of relating efficacy measures to unbound drug concentrations for anti-infective agents, Clin. Microbiol. Rev. 26 (2013) 274–288.
[44] B. Bhattacharya, S. Nakka, L. Guruprasad, A. Samanta, Interaction of bovine serum albumin with dipolar molecules: fluorescence and molecular docking studies, J. Phys. Chem. B 113 (2009) 2143–2150.
[45] C. Esterhuysen, A. Hesselmann, T. Clark, Trifluoromethyl: an amphiphilic noncovalent bonding partner, Chemphyschem 18 (2017) 772–784.
[46] D. Musumeci, G.N. Roviello, G. Rigione, D. Capasso, S. Di Gaetano, C. Riccardi, V. Roviello, D. Montesarchio, Benzodifuran derivatives as potential antiproliferative agents: possible correlation between their bioactivity and aggregation properties, ChemPlusChem 82 (2017) 251–260.
[47] K. Gaur, A.M. Vázquez-Salgado, G. Duran-Camacho, I. Dominguez-Martinez, J.A. Benjamín-Rivera, L. Fernández-Vega, L.C. Sarabia, A.C. García, F. Pérez-Deliz, J.A.M. Román, M. Vega-Cartagena, S.A. Loza-Rosas, X.R. Acevedo, A.D. Tinoco, Iron and copper intracellular chelation as an anticancer drug strategy, Inorganics 6 (2018) 126–163.
[48] G.N. Roviello, C. Vicidomini, V. Costanzo, V. Roviello, Nucleic acid binding and other biomedical properties of artificial oligolysines, Int. J. Nanomedicine 11 (2016) 5897–5904.